Subpixel Land Cover Mapping by Integrating Spectral and Spatial Information of Remotely Sensed Imagery

Feng Ling, Yun Du, Fei Xiao, and Xiaodong Li

***Abstract*—Subpixel mapping (SPM) is a technique to predict spatial locations of land cover classes within mixed pixels in remotely sensed imagery. The two-step approach first estimates fraction images by spectral unmixing and then inputs fraction images into an SPM algorithm to generate the final subpixel land cover map. A shortcoming of this approach is that the information about the credibility of fraction images is not considered. In this letter, we proposed a general framework of SPM which is directly applied to original coarse resolution remotely sensed imagery by integrating spectral and spatial information. Based on the proposed framework, the linear unmixing model and the maximal spatial dependence model were combined to construct a novel SPM model aiming to minimize the least squares error of spectral signature and make the subpixel land cover map spatially smooth, simultaneously. By applying to an Airborne Visible/Infrared Imaging Spectrometer hyperspectral image, the proposed model was evaluated both visually and quantitatively by comparing it with hard classification and the two-step SPM approach. The results showed that the regularization parameter, which balances the influence of spectral and spatial terms, plays an important role on the solution. The L-curve approach was a reasonable method to select the regularization parameter, with which an increased accuracy of the proposed model was obtained.**

***Index Terms*—Mixed pixel, spectral unmixing, subpixel mapping (SPM), superresolution.**

I. Introduction

SUBPIXEL mapping (SPM), which can be considered as the postprocessing of spectral unmixing, is a technique to retrieve a subpixel land cover map with finer spatial resolution than the original image using fraction images yielded by spectral unmixing as input [1], [2]. In general, SPM is solved based on spatial dependence, i.e., the tendency for spatially proximate observations of a given property to be more similar than that of more distant observations. In this condition, SPM can be formulated as an optimization model to maximize the spatial dependence while maintaining land cover fractions. Many algorithms have been proposed to address this problem, such as Hopfield neural network [3]–[5], linear optimization [6], genetic algorithm [7], and pixel swapping [8].

Manuscript received June 13, 2011; revised August 25, 2011; accepted September 16, 2011. This work was supported in part by the Natural Science Foundation of China under Grant 40801186 and in part by the Wuhan Youth Chenguang Project under Grant 200950431218.

The authors are with the Institute of Geodesy and Geophysics, Chinese Academy of Sciences, Wuhan 430077, China (e-mail: lingf@whigg.ac.cn; duyun@whigg.ac.cn; xiaof@whigg.ac.cn; lixiaodong@whigg.ac.cn).

Digital Object Identifier 10.1109/LGRS.2011.2169934

In practice, the two-step approach (SPM_TSA), which first estimates fraction images by spectral unmixing and then inputs fraction images into an SPM algorithm to generate the final subpixel land cover map, is commonly used [9]–[14]. Although SPM_TSA is simple and intuitive, it is constrained not only by the SPM algorithm but also by the spectral unmixing algorithm used to estimate inputted fraction images.

Given that spectral unmixing is still an open problem and accurate fraction images are always unavailable [15], [16], the information about the credibility of fraction images is necessary to fully describe the result of spectral unmixing [17]. When SPM_TSA is applied, however, only fraction images are used in the latter SPM algorithm, and no information about their uncertainty is considered. This is an obvious shortcoming of SPM_TSA. Because the uncertainty of fraction images is determined by spectral signatures of endmembers and target mixed pixels, incorporating spectral information into the SPM procedure is then expected to handle the uncertainty.

The object of this letter is to propose a general framework of SPM by integrating spectral and spatial information of remotely sensed imagery. It will be also shown how this framework can be implemented with certain spectral unmixing and spatial mapping models. The main advantage of this framework is that the uncertainty of fraction images, which is represented by the spectral residual, is considered when the final subpixel land cover map is directly retrieved from original remotely sensed imagery.

The remainder of this letter is organized as follows. Section II briefly describes the background of spectral unmixing and SPM. Section III introduces the proposed framework. Section IV presents qualitative and quantitative experimental results. Section V concludes with some remarks.

II. Background

Let y be the observed multispectral remotely sensed image with L bands of coarse resolution R_y, and y has $N_{yr} \times N_{yc}$ pixels. By setting the zoom factor to be z, SPM aims to generate a labeled land cover map at the finer resolution R_x, which is set to be R_y/z. Suppose that the number of land cover classes in the entire image is C, then, the final subpixel land cover map x contains $(z \times N_{yr}) \times (z \times N_{yc})$ subpixels, whose labels can be defined to a unique class of C.

To solve the aforementioned SPM problem, the commonly used approach necessitates two steps. First, the abundance of each land cover class in each pixel is obtained by spectral

unmixing. Then, according to the spatial pattern of land cover classes, the final subpixel land cover map is generated using fraction images as input. In this letter, linear unmixing model (LUM) is used for spectral unmixing, and the maximal spatial dependence model is adopted for SPM, which are briefly introduced in the following sections.

A. Spectral Unmixing

The object of spectral unmixing is to extract fraction images of original coarse resolution imagery. In general, LUM views spectral signatures of each mixed pixel as being made up of a weighted linear sum of spectral signatures of endmembers within that pixel. The weights are determined by the relative area proportions of each endmember [18].

Let r be an $L \times 1$ column pixel vector in the multispectral image y. Assume that $t_1, t_2, \ldots, t_c$ are C land cover classes in the image and M is the signature matrix denoted by $[m_1, m_2, \ldots, m_c]$, where m_i is an $L \times 1$ column vector represented by the signature of the ith target t_i. Furthermore, assume that $\alpha = (\alpha_1, \alpha_2, \ldots, \alpha_c)^T$ is a $C \times 1$ abundance column vector associated with r, where α_j denotes the area fraction of the jth land cover classes in r. The pixel vector r is modeled as a linear mixture of target signature

$$r = M\alpha + n \tag{1}$$

where n is the residual term representing the noise or the measurement error.

In order to make the estimated fractions physically meaningful, LUM is always subject to two constraints on the entries of α. First, the nonnegativity condition requires all fractions to be nonnegative. Second, the full additivity condition requires all fractions in a mixed pixel to be subject to the unity constraint. To extract fractions of all endmembers, LUM is considered as an optimization model aiming to minimize the least squares error of spectral signature, which is mathematically expressed as

$$\text{Min } LS = (r - M\alpha)^T (r - M\alpha) \tag{2}$$

Subject to :

$$\alpha_i \geq 0,\ i = 1, \ldots, C \tag{3}$$

$$\sum_{i=1}^{C} \alpha_i = 1 \tag{4}$$

B. SPM

SPM aims to maximize the spatial dependence while maintaining the input fractions of each land cover class in all pixels, and it can be formulated as an optimization model

$$\text{Max } SD = \sum_{y} \sum_{i=1}^{z^2} \sum_{c=1}^{C} x_{ic} * d_{ic} \tag{5}$$

$$x_{ic} = \begin{cases} 1 & \text{if subpixel } i \text{ is assigned to} \\ & \quad \text{land cover class } c \\ 0 & \text{otherwise} \end{cases} \tag{6}$$

$$\text{Subject to : } \sum_{c=1}^{C} x_{ic} = 1 \tag{7}$$

$$\sum_{i=1}^{z^2} x_{ic} = N_{SP}^{c} \tag{8}$$

where d_{ic} is the measurement of spatial dependence for subpixel i when it is assigned to the land cover class c. The first constraint in (7) aims to make all subpixels only belong to one certain class. The area constraint in (8) ensures that the number of subpixels for the land cover class c agrees with N_{SP}^{c}, which is determined by the area fraction and the zoom factor z as

$$N_{SP}^{c} = \alpha_c \cdot z^2. \tag{9}$$

In general, d_{ic} can be computed as a distance-weighted function in terms of its subpixel neighbors

$$d_{ic} = \sum_{j=1}^{N'} \lambda_{ij} Z_c(p_j) \tag{10}$$

$$\lambda_{ij} = \exp(-h_{ij}/w) \tag{11}$$

where N' is the number of subpixel neighbors, $Z_c(p_j)$ is the value of the class c (constrained to be either zero or one) of subpixel p_j, λ_{ij} is a distance-dependent weight, h_{ij} is the distance between subpixel p_i (for which the spatial dependence is desired) and the neighboring subpixel p_j, and w is the nonlinear parameter of the distance-decay model.

III. Methodology

For each subpixel land cover configuration within a mixed pixel, the spectral signature of this mixed pixel can be simulated as a combination of the subpixel spectral signatures of the pixel's components. From this perspective, meeting the condition of the area constraint in SPM is identical to minimizing the difference between the simulated spectral signature and the actual spectral signature of the mixed pixel, which is also the object of spectral unmixing. Therefore, SPM can be formulated as a multiobject optimization problem aiming to maximize the spatial dependence and make fraction images of the final subpixel land cover map satisfy the criterion of one certain spectral unmixing model.

We then propose a general SPM framework, in which both spectral and spatial goal functions are combined to form a single optimization function

$$\text{Min } E(r) = E_{\text{spectral}}(r) + \lambda \cdot E_{\text{spatial}}(r). \tag{12}$$

The first term $E_{\text{spectral}}(r)$ aims to match the spectral information provided by mixed pixels. The second term $E_{\text{spatial}}(r)$ aims to match the prior spatial land cover pattern model. The parameter λ is used to balance the impact of spectral and spatial terms on the final goal function. Once the spectral model and the spatial model are determined, a certain SPM model can be constructed based on the proposed framework. It should be noticed that the Markov-random-field-based SPM model [19], [20], which uses the Gaussian maximum likelihood method to

simulate the spectral term and uses the Markov random field to represent the spatial term, is a stochastic model generated with Bayesian methods under this framework.

In this letter, we construct a novel deterministic SPM model by combining the Linear Unmixing Model and the Maximum Spatial Dependence Model (SPM_LM) based on the proposed framework. SPM_LM aims to minimize a weighted sum of spectral and spatial terms, which is mathematically expressed as

$$\text{Min } E = \sum_{y}(r - M\alpha)^T(r - M\alpha) + \lambda \cdot \sum_{y}\sum_{i=1}^{z^2}\sum_{c=1}^{C} x_{ic} * d'_{ic} \tag{13}$$

subject to :

$$\alpha_c = \sum_{i=1}^{z^2}\sum_{c=1}^{C} x_{ic} \Big/ z^2 \tag{14}$$

$$\sum_{c=1}^{C} x_{ic} = 1 \tag{15}$$

$$d'_{ic} = -d_{ic}. \tag{16}$$

The first term of the SPM_LM model is the spectral term, which is indeed the object function of LUM. Both constraints of LUM as in (3) and (4) are automatically satisfied in SPM_LM once (14) and (15) are satisfied. Equation (14) makes the sum of area percentages of land cover classes equal to one, and the constraint in (15) that each subpixel belongs to only one land cover class makes the area percentage of each land cover class not less than zero.

The second term of the SPM_LM model is the spatial term, which is the object function for spatial mapping. Because the object of SPM_LM is finding the minimum value, (16) is used here to make the maximal spatial dependence contribute the minimal value.

Maximizing the land cover spatial dependence is identical to making the resulting land cover map spatially smooth, and the proposed framework can then be considered essentially as a regularization method for an ill-posed problem [21], [22]. From this viewpoint, the spectral term is the data term to persevere information of the original image, and the spatial term is the regularization term aiming to make the solution smooth.

The regularization parameter λ acts as a tradeoff parameter to balance the influence of the spectral term and the spatial term in the final solution of (13). If the regularization parameter is too small, the solution is unsmoothed and susceptible to noise in the original image. On the other hand, if the regularization parameter is too large, the spatial term will have a dominating effect on the solution and make the final subpixel land cover map oversmoothed. Therefore, there needs to be a proper balance of the spectral term and the spatial term when SPM_LM is implemented. In this letter, the widely used L-curve approach [23], [24] is used to find the optimal value of the regularization parameter λ.

The simulated annealing algorithm [20] is used to achieve the global minima of SPM_LM. Land cover class labels of subpixels are iteratively changed to minimize the value of E in (13). The annealing schedule is defined on the basis of a power-law decay function, where temperature T at the iteration n is modified according to

$$T_n = \sigma \cdot T_{n-1}. \tag{17}$$

The parameter $\sigma \in (0, 1)$ controls the rate of temperature decrease, and the algorithm is implemented through the following steps.

1) Randomly label all subpixels within each coarse pixel. Set the maximum iteration number $ite_{\max}$, the starting temperature T_0, and the parameter σ.
2) All the subpixel labels are updated using the Metropolis–Hastings sampler [25]. The number of successful updates is then counted.
3) End iteration if $ite \geq ite_{\max}$ or the number of successful updates is lower than 0.1% of the total number of pixels after three consecutive iterations; otherwise, step 2 is repeated.

IV. Experiments and Result Analysis

In this section, the performance of SPM_LM was validated by comparison with hard classification and SPM_TSA, in which the constrained linear spectral unmixing algorithm [18] was applied for spectral unmixing and the pixel swapping algorithm [8] was adopted for SPM. The Kappa coefficients of final subpixel land cover maps were used to validate the SPM_LM model quantitatively. Moreover, the root-mean-square error (rmse) of area fractions for different land cover classes between final subpixel land cover maps and the referent map was used to judge if the error of fraction images generated by spectral unmixing could be eliminated.

The test data set is from an Airborne Visible/Infrared Imaging Spectrometer (AVIRIS) image taken over northwest Indiana's Indian Pine test site in June 1992. A small part of the scene consisting of 64 × 64 pixels was considered. The original AVIRIS image was spatially degraded by averaging pixel values to simulate coarse spatial resolution images. In this experiment, two coarse spatial resolution images were derived by zoom factors of four and eight from the original 20-m resolution image [Fig. 1(a)] to spatial resolutions of 80 m [Fig. 1(b)] and 160 m [Fig. 1(c)]. Assuming the original 20-m-resolution AVIRIS image pixels to be pure pixels, the fine resolution land cover map, which contains four land cover classes (water, corn, wheat, and woods) as shown in Fig. 1(d), was extracted from the original image by manually digitizing it and using it as the reference.

In this experiment, a total of 20 bands of noisy channels and water absorption channels of the AVIRIS image were removed. The remaining 200 spectral channels were used. Representative pixels of four endmembers were manually selected from the image scene, and their average was used to represent the endmember signature. It should be noted that some methods aiming to improve efficiency of spectral unmixing can be used in SPM_LM, such as reducing the dimension of the data and selecting different endmembers for one land cover class [16]. However, the discussion about the effect of these technologies

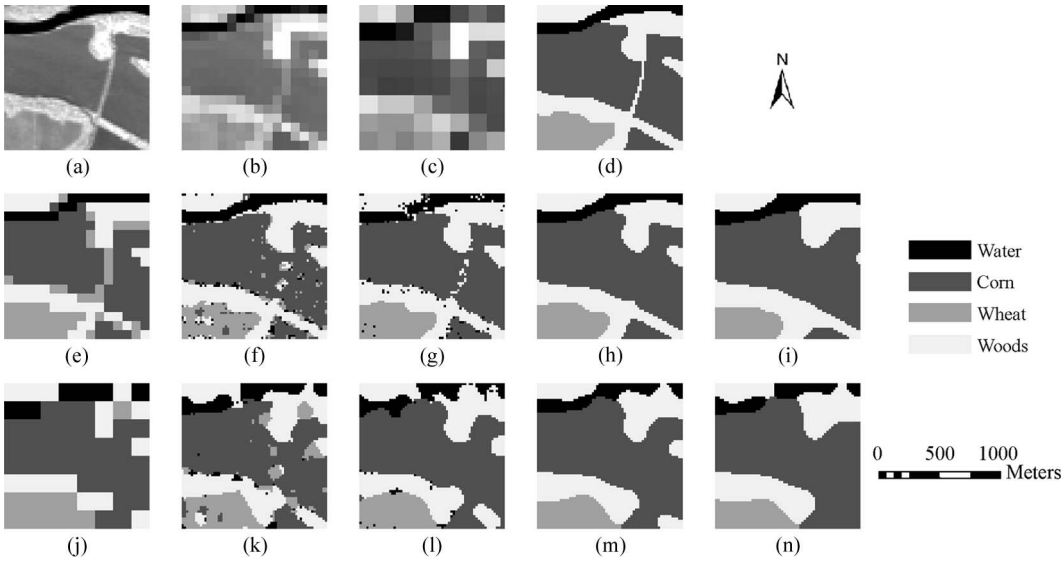

Fig. 1. SPM results of the AVIRIS image. (a) Forty-first band of AVIRIS at the 20-m spatial resolution (64 × 64 pixels). (b) Degraded AVIRIS image at the 80-m spatial resolution (16 × 16 pixels). (c) Degraded AVIRIS image at the 160-m spatial resolution (8 × 8 pixels). (d) Reference high-resolution land cover map. (e)–(i) Land cover maps of (b) generated by hard classification, SPM_TSA, and SPM_LM with $\lambda^{0.1L}$, λ^{L}, and λ^{10L}, respectively. (j)–(n) Land cover maps of (c) generated by hard classification, SPM_TSA, and SPM_LM with $\lambda^{0.1L}$, λ^{L}, and λ^{10L}, respectively.

on the final result is beyond the scope of this research, and we only used the simple method to choose the endmember in this experiment without using dimensionality reduction techniques.

Once the endmembers are determined, the final subpixel land cover map can be generated by SPM_LM without training samples. The annealing schedule proposed in [20] was used, and the convergence iteration times depend on the zoom factor and the number of bands. All algorithms were tested on Intel Core 2 Processor, 2.66 GHz Duo CPU with 1.98 GB RAM using MATLAB 7.3 version. In our experiments for the zoom factor $z = 4$, convergence is reached in less than 60 iterations using about 55 s for SPM_LM, while convergence is reached using about 15 s for SPM_TSA.

We first determined the value of λ with the L-curve approach. We ran SPM_LM with different values of λ and found the optimal value of λ with MATLAB tools provided by Hansen [24]. To illustrate the influence of regularization parameter, we generated three subpixel land cover maps with different values of λ, including the value of λ chosen by L-curve (λ^{L}) and the values of λ having one tenth and ten times of λ^{L} (shown as $\lambda^{0.1L}$ and λ^{10L}, respectively). Moreover, land cover maps of hard classification generated by the spectral angle mapper algorithm were also used for comparison. All resulting land cover maps are displayed in Fig. 1(e)–(n) with zoom factors $z = 4$ and $z = 8$, respectively.

Visual comparison of results shows that SPM provided more detailed information than hard classification. Hard classification can only generate land cover maps at the pixel scale, and a considerable amount of land cover information within pixels is lost. On the contrary, SPM can recover the land cover information at the subpixel scale to a great extent. For SPM approaches, SPM_LM prevails over SPM_TSA compared with the reference land cover map shown in Fig. 1(d). It is noticed that results of SPM_TSA have many isolated patches caused by spectral unmixing errors. For SPM_LM, isolated patches still exist when $\lambda^{0.1L}$ is adopted, while with λ^{10L}, land cover patches become too rounded to represent their original characteristics. In comparison, λ^{L} makes a good balance between eliminating spectral unmixing errors and avoiding oversmoothed. Almost all isolated patches are eliminated while boundaries between different land cover classes are properly reconstructed.

TABLE I
RMSE OF FRACTION IMAGES AND KAPPA COEFFICIENTS OF RESULTING LAND COVER MAPS WITH DIFFERENT METHODS FOR THE AVIRIS IMAGE

			Hard	SPM_TSA	SPM_LM			
					$\lambda^{0.1L}$	λ^{L}	λ^{10L}	λ^{HK}
Z=4	RMSE	Water	0.070	0.051	0.040	0.023	0.069	0.027
		Corn	0.195	0.106	0.063	0.071	0.156	0.066
		Wheat	0.311	0.105	0.021	0.044	0.097	0.044
		Woods	0.189	0.083	0.065	0.088	0.193	0.085
	Kappa		0.787	0.830	0.903	0.937	0.862	0.939
Z=8	RMSE	Water	0.148	0.038	0.030	0.024	0.021	0.027
		Corn	0.167	0.099	0.055	0.077	0.155	0.077
		Wheat	0.187	0.143	0.048	0.082	0.098	0.082
		Woods	0.241	0.085	0.074	0.119	0.187	0.119
	Kappa		0.736	0.741	0.807	0.823	0.776	0.827

Accuracy measures of these approaches are shown in Table I. Among the subpixel maps generated by SPM_LM with different values of λ ranging from $\lambda^{0.1L}$ to λ^{10L}, the subpixel map with λ value of λ^{HK}, which was chosen in terms of the highest Kappa coefficient, was also used for comparison. The result of SPM_LM with λ^{L} shows a good performance. RMSE values of λ^{L} are lower than those of $\lambda^{0.1L}$ and λ^{10L}, while Kappa coefficient of λ^{L} is higher than that of $\lambda^{0.1L}$ and λ^{10L}. Moreover, Kappa coefficient values of λ^{L} are only 0.002 and 0.004 lower than those of λ^{HK} at $z = 4$ and $z = 8$. RMSE values of λ^{L} are close to those of λ^{HK}, and even several rmse values of λ^{L} are lower.

A great improvement is noticed for SPM_LM compared with hard classification and SPM_TSA. For the zoom factor $z = 4$, the Kappa coefficient increases by 0.15 and 0.107 for λ^L, and even with values of $\lambda^{0.1L}$ and λ^{10L}, the improvement is still obvious. A similar trend is noticed for the zoom factor $z = 8$, although the improvement is different. RMSE values of SPM_LM with λ^L are lower than those of hard classification and SPM_TSA, except the "woods" class of SPM_TSA, which is mainly caused by the linear feature of woods.

V. Conclusion

In this letter, we have proposed a framework for subpixel land cover mapping of remotely sensed imagery. This framework incorporates the spectral information in remotely sensed images directly into the spatial mapping procedure, and both spectral information and spatial information of remotely sensed imagery are combined to one optimization model. We used the LUM and the maximal spatial dependence model to construct a novel SPM model within the proposed framework. We found the optimal solution of the proposed SPM_LM model with the simulated annealing algorithm and selected the regularization parameter by the L-curve approach.

For an experimental study, an AVIRIS hyperspectral image was used to test the efficacy of the proposed SPM_LM model. The results showed that the value of the regularization parameter played an important role on the solution, and the L-curve approach was a reasonable method to select the optimal value of regularization parameter. With the L-curve approach, the final subpixel land cover map has a significant increase in the accuracy over that produced by hard classification and the two-step approach.

Although this proposed framework has evident advantage than the two-step approach, other possibilities for improvement exist. For example, different spectral unmixing models can be combined with different spatial pattern description to generate various models under this framework. The regularization parameter value selection method is also needed to be further studied.

Acknowledgment

The AVIRIS image used in this study was downloaded from http://dynamo.ecn.purdue.edu/~biehl/. The authors would like to thank the reviewers for their valuable comments.

References

[1] A. J. Tatem, H. G. Lewis, P. M. Atkinson, and M. S. Nixon, "Super-resolution target identification from remotely sensed images using a Hopfield neural network," *IEEE Trans. Geosci. Remote Sens.*, vol. 39, no. 4, pp. 781–796, Apr. 2001.

[2] P. M. Atkinson, "Issues of uncertainty in super-resolution mapping and their implications for the design of an inter-comparison study," *Int. J. Remote Sens.*, vol. 30, no. 20, pp. 5293–5308, Oct. 2009.

[3] A. J. Tatem, H. G. Lewis, P. M. Atkinson, and M. S. Nixon, "Super-resolution land cover pattern prediction using a Hopfield neural network," *Remote Sens. Environ.*, vol. 79, no. 1, pp. 1–14, Jan. 2002.

[4] M. Q. Nguyen, P. M. Atkinson, and H. G. Lewis, "Superresolution mapping using a Hopfield neural network with fused images," *IEEE Trans. Geosci. Remote Sens.*, vol. 44, no. 3, pp. 736–749, Mar. 2006.

[5] F. Ling, Y. Du, F. Xiao, H. Xue, and S. Wu, "Super-resolution land-cover mapping using multiple sub-pixel shifted remotely sensed images," *Int. J. Remote Sens.*, vol. 31, no. 19, pp. 5023–5040, Sep. 2010.

[6] J. Verhoeye and R. De Wulf, "Land cover mapping at sub-pixel scales using linear optimization techniques," *Remote Sens. Environ.*, vol. 79, no. 1, pp. 96–104, Jan. 2002.

[7] K. C. Mertens, L. P. C. Verbeke, E. I. Ducheyne, and R. De Wulf, "Using genetic algorithms in sub-pixel mapping," *Int. J. Remote Sens.*, vol. 24, no. 21, pp. 4241–4247, Nov. 2003.

[8] P. M. Atkinson, "Sub-pixel target mapping from soft-classified remotely sensed imagery," *Photogramm. Eng. Remote Sens.*, vol. 71, no. 7, pp. 839–846, Jul. 2005.

[9] G. M. Foody, "The role of soft classification techniques in the refinement of estimates of ground control point location," *Photogramm. Eng. Remote Sens.*, vol. 68, no. 9, pp. 897–903, Sep. 2002.

[10] G. M. Foody, A. M. Muslim, and P. M. Atkinson, "Super-resolution mapping of the waterline from remotely sensed data," *Int. J. Remote Sens.*, vol. 26, no. 24, pp. 5381–5392, Dec. 2005.

[11] M. Q. Nguyen, P. M. Atkinson, and H. G. Lewis, "Superresolution mapping using a Hopfield neural network with LIDAR data," *IEEE Geosci. Remote Sens. Lett.*, vol. 2, no. 3, pp. 366–370, Jul. 2005.

[12] M. W. Thornton, P. M. Atkinson, and D. A. Holland, "Sub-pixel mapping of rural land cover objects from fine spatial resolution satellite sensor imagery using super-resolution swapping," *Int. J. Remote Sens.*, vol. 27, no. 3, pp. 473–491, Feb. 2006.

[13] F. Ling, F. Xiao, Y. Du, H. P. Xue, and X. Y. Ren, "Waterline mapping at the subpixel scale from remote sensing imagery with high-resolution digital elevation models," *Int. J. Remote Sens.*, vol. 29, no. 6, pp. 1809–1815, Mar. 2008.

[14] F. Ling, W. B. Li, Y. Du, and X. Li, "Land cover change mapping at the subpixel scale with different spatial-resolution remotely sensed imagery," *IEEE Geosci. Remote Sens. Lett.*, vol. 8, no. 1, pp. 182–186, Jan. 2011.

[15] L. Bastin, "Comparison of fuzzy c-means classification, linear mixture modelling and MLC probabilities as tools for unmixing coarse pixels," *Int. J. Remote Sens.*, vol. 18, no. 17, pp. 3629–3648, Nov. 1997.

[16] N. Keshava and J. F. Mustard, "Spectral unmixing," *IEEE Signal Process. Mag.*, vol. 19, no. 1, pp. 44–57, Jan. 2002.

[17] G. M. Foody and H. T. X. Doan, "Variability in soft classification prediction and its implications for sub-pixel scale change detection and super resolution mapping," *Photogramm. Eng. Remote Sens.*, vol. 73, no. 8, pp. 923–933, Aug. 2007.

[18] D. C. Heinz and C. I. Chang, "Fully constrained least squares linear spectral mixture analysis method for material quantification in hyperspectral imagery," *IEEE Trans. Geosci. Remote Sens.*, vol. 39, no. 3, pp. 529–545, Mar. 2001.

[19] T. Kasetkasem, M. K. Arora, and P. K. Varshney, "Super-resolution land cover mapping using a Markov random field based approach," *Remote Sens. Environ.*, vol. 96, no. 3/4, pp. 302–314, Jun. 2005.

[20] V. Tolpekin and A. Stein, "Quantification of the effects of land-cover-class spectral separability on the accuracy of Markov-random-field-based superresolution mapping," *IEEE Trans. Geosci. Remote Sens.*, vol. 47, no. 9, pp. 3283–3297, Sep. 2009.

[21] D. Calvetti, S. Morigi, L. Reichel, and F. Sgallari, "Tikhonov regularization and the L-curve for large discrete ill-posed problems," *J. Comput. Appl. Math.*, vol. 123, no. 1/2, pp. 423–446, Nov. 2000.

[22] S. Farsiu, M. D. Robinson, M. Elad, and P. Milanfar, "Fast and robust multiframe super resolution," *IEEE Trans. Image Process.*, vol. 13, no. 10, pp. 1327–1344, Oct. 2004.

[23] P. C. Hansen and D. P. Oleary, "The use of the L-curve in the regularization of discrete ill-posed problems," *SIAM J. Sci. Comput.*, vol. 14, no. 6, pp. 1487–1503, Nov. 1993.

[24] P. C. Hansen, "Regularization tools version 4.0 for MATLAB 7.3," *Numer. Algorithms*, vol. 46, no. 2, pp. 189–194, Oct. 2007.

[25] S. Geman and D. Geman, "Stochastic relaxation, Gibbs distributions, and the Bayesian restoration of images," *IEEE Trans. Pattern Anal. Mach. Intell.*, vol. PAMI-6, no. 6, pp. 721–741, Nov. 1984.